Study of Weld Geometry, Microstructure and Hardness of Fibre Laser Welded Dual Phase Steel

P V S Lakshminarayana[1,2*], Jai Prakash Gautam[2], P. Mastanaiah[3], G. Madhusudan Reddy[4], K Bhanu Sankara Rao[1]

[1] Department of Metallurgical and Materials Engineering, Mahatma Gandhi Institute of Technology, Gandipet, CBES P.O. Hyderabad- 500075.

[2] SEST, University of Hyderabad

[3] DRDL, Hyderabad, [4]Defence Metallurgical Research Laboratory, Hyderabad

[*] corresponding author email: laxmanpv1@gmail.com

DOI : 10.22486/iwj/2019/v52/i4/186785

ABSTRACT

Laser weld beads were produced on Dual Phase 600 grade steel sheets of 1.6 mm thickness using Nd: YAG fibre lasers. Influence of welding speed and laser beam power on variations in the weld geometry and Microstructure, and its correlation with the mechanical properties was studied. Welding speed has a greater influence on the width of the weld zone and Heat Affected Zone, and depth of penetration than beam power. Rapid cooling rates associated with the weld zone resulted in the formation of martensite phase and a decrease in the volume fraction of martensite was observed with an increase in the distance from the weld zone. Microhardness of the weld zone increased to 360 - 380 HV from 180 - 200 HV.

Keywords: Dual Phase Steel; Fibre Laser Welding; Fusion Zone; Heat Affected Zone; Beam Power; Traverse Speed.

1.0 INTRODUCTION

Extensive research has been taken place over the decade by the steel industry to develop a new class of material for the automobile industry to meet the functional and environmental requirements. The conventional structural and body materials of automobiles have been replaced by Advanced High Strength (AHS) Steels, as these are having superior mechanical properties and also suitable to meet the modern environmental standards [1]. Among the AHS steels, Dual Phase Steels, 1st generation of AHS Steels family, have attracted the attention of researchers and end-users because of its excellent toughness, high initial work hardening rate, low ratio of yield strength to ultimate tensile strength without any evidence of yield point phenomenon, excellent formability, and easy to manufacture [2]. The proportion of application of DP steels, as automobile body structure, has increased to an extent 40 % over a decade by replacing mild steel [1]. DP Steels consist of soft ferrite matrix embedded with hard martensite matrix to an extent of 15-25% [3-4]. Also, the microstructure consists of retained austenite (RA) and Bainite in smaller proportions beside ferrite and martensite. Mechanical properties of dual phase steels are mainly depending on microstructural constituents i.e., the volume fraction of martensite and ferritic grain refinement. With the increasing martensite content, strength of the steel increases at the cost of ductility. Also, strength of the steel increases with grain refinement of ferrite and formation of substructure [5]. Fibrous morphology of martensite with finer size shows better ductility and strength than other morphologies [6].

Welding has become one of the primary manufacturing steps in the production (assembly) of an automobile body. Producing body-in-white components by joining these DP steels with other materials keeping minimum distortion in the structure is possible with laser welding due to minimum sizes of weld zone and Heat Affected Zone than other welding Methods [7]. Laser welding technique has created its mark in the automobile industry due to its processing speed, high power density, the flexibility of the laser spot to weld the intricate shapes of the components [8]. The usage of optical fibres for delivering the lasers has gained industrial applications because of its higher efficiency, precision, high power density, small beam divergence, and small focal spot diameter with cost-effectiveness [9]; with these improvements, producing a narrower width of Heat Affected Zone (HAZ) and Weld Zone (WZ) have become easier with fibre lasers.

Mechanical properties and variation of the microstructure of the laser weld joints are being influenced by Laser beam power, shielding gas flow rate, welding speed, and laser spot diameter [10-13]. In the present work, influence of laser beam power and traverse (welding) speed on the variation of micro-structure, weld geometry, and variation of hardness have been studied by producing beads on a plate on DP Steel of 590 grade.

2.0 EXPERIMENTAL STUDIES

The DP 590 grade steel of 100 mm x 120 mm x 1.6 mm thickness sheet was used in the present work. This steel consists of (average weight %) C-0.083 %, Mn – 1.71%, Si – 0.4 %, and Cr – 0.01%. The tensile strength of as received DP 590 steel sheet is given as 610 ± 10 MPa and yield strength is given as 350 ± 10 MPa with an elongation of 28-30%. Prior to welding, surface cleaning was carried out by mechanical polishing and alcohol cleaning. Weld beads were produced perpendicular to the rolling direction.

The laser generator used in this investigation was an Arnold Nd-Ytterbium doped fibre laser. The focal length and fibre core diameter were 300 mm and 0.02 mm respectively. The laser head was at 90° to the specimen surface and the welding was carried out in keyhole mode. Weld beads were produced by varying the parameters of welding speed and Laser beam power. The details are given in **Table 1**. Specimens were cut in the transverse direction to the weld bead to study the variation of microstructure in Heat Affected Zone (HAZ) and Weld Zone (WZ) with reference to the base material and the hardness variations in these zones and their correlation. Specimens were prepared for microscopic examination by the standard polishing procedure followed by diamond paste polishing. The prepared samples were etched with 2% Nital solution.

Table 1 : Weld Parameters used to produce beads on DP 600

Sl. No.	Laser Beam Power, W	Welding Speed mm/min	Heat Input per unit length J/mm
1	2500	2000	75
2		4000	37.5
3		6000	25
1	3500	2000	105
2		4000	52.5
3		6000	35

Olympus BX-51M was used to study microstructural variation across the weld joint. Microhardness profile was measured from the base material to base material through Heat Affected Zone and Weld Zone at a load of 500g with 15s dwell time. The distance between each indentation was 0.2 mm. Enough distance was maintained between each indentation to avoid the work hardening effect.

3.0 RESULTS AND DISCUSSION

Fig. 1 shows the microstructure of the weld joints at both laser beam powers of 2500 W and 3500 W and at a welding speed of 2000 mm/min, 4000 mm/min, and 6000 mm/min. For easy identification and traceability, nomenclature to the weld beads are given according to the corresponding laser beam power and welding speed like BW - XYA, where BW indicates Bead on Weld, XY indicates laser beam power in kW and A indicates welding speed in m/mm.

From **Fig. 1**, it has been observed that the resultant weld structures are free from micro-defects such as voids, cracks and gas holes. The growth of the fusion zone has been initiated from the boundary of the fusion and proceeds towards the central line of the weld resulting in the formation of columnar dendritic structure and the symmetry has been observed with the weld central line.

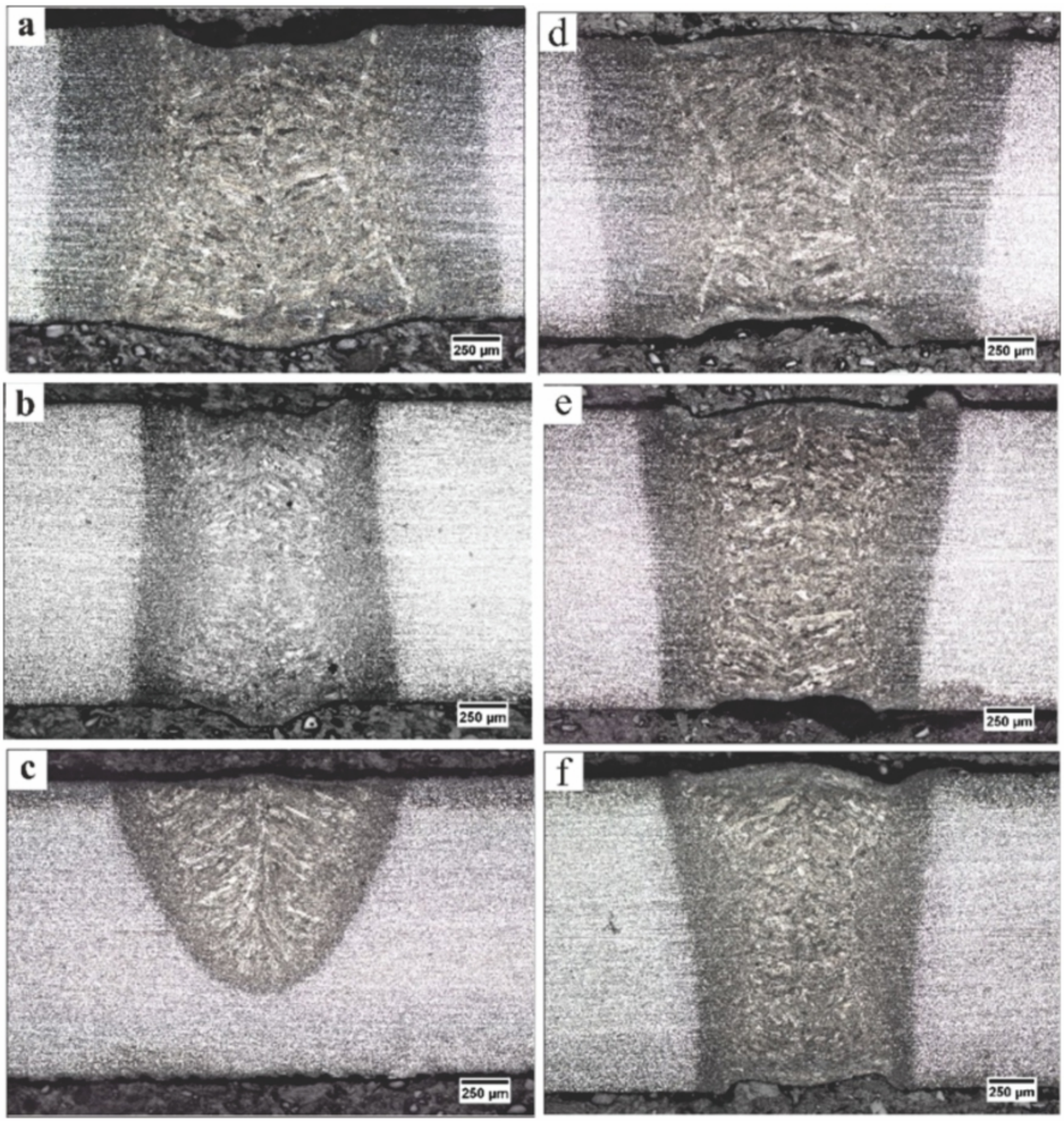

Fig. 1 : Micrographs of weld structures of 2500 W and 3500 W [(a-c): 2500 W and 2000, 4000 & 6000 mm/min, (d-f): 3500 W and 2000, 4000 & 6000 mm/min]

Weld parameters, i.e., Laser beam power (BP) and Welding Speed (WS) have a greater influence on the depth of penetration and widths of weld zone (WZ) and Heat Affected Zone. BP influences the quantity of liquid metal produced and WS will influence the rate of solidification of the weld pool [14]. **Fig. 1(a-c)** show microstructures of weld beads produced at the constant BP of 2500W and (d-f) show the microstructures at the constant BP of 3500 W by varying the WS as 2000 mm/min, 4000 mm/min, and 6000 mm/min respectively at both laser beam powers. It is observed from **Fig. 1** that the complete depth of penetration has been achieved for all the weld beads expect for BW-256. The partial penetration for BW-256 is mainly attributed to the higher traverse speed (6000 mm/min) at the beam power of 2500 as higher welding speeds decrease the Heat Input per Unit Length (HI) at the same beam power. For BW-256, the HI was 25 J/mm which was not enough for complete penetration. However, for the same beam power at lower welding speeds (4000 mm/min and 2000 mm/min) complete penetration has been observed may be due to the higher HI (37.5 J/mm and 75 J/mm). Also, at the same traverse speed (6000 mm/min), with an increase in laser beam power to 3500 W complete penetration has been observed with BW-356 as there has been an improvement in the HI from 25 J/mm to 35 J/mm [15].

Width of weld zone and HAZ have been influenced by Laser beam power and welding speed. It was observed from **Fig. 1** that widths of WZ and HAZ have decreased, as welding speed is decreased at the constant beam power. Also, observed that weld joints dimensions have increased with increasing the beam power at constant welding speed. Dimensions of the weld zone and HAZ were measured using ImageJ software. The graphical representation of the relation between the weld joint dimensions and the heat input per unit length is given in **Fig. 2**.

It is observed from **Fig. 2** that with increasing heat input per unit length, width of the HAZ and WZ have increased. Higher width of WZ and HAZ have been observed for the Heat input of 75 J/mm and 105 J/mm whereas lower weld joint dimensions have been observed for the Heat Input of 35 J/mm and 37.5 J/mm. During solidification of the weld pool excess heat energy of the weld pool has been dissipated to the surrounding material and heated up the material adjacent to the weld zone by which HAZ has formed. Higher the rate of solidification, faster is the dissipation of heat energy to the surrounding material. From **Fig. 2**, it is observed that at a beam power of 2500 W with increasing the welding speed from 2000 mm/min to 4000 mm/min an appreciable decrease in the weld joint dimensions has been observed. Similar relation has been found with 3500 W, as welding speed increased. From **Fig. 2**, it is concluded that BW-254 has minimum weld joint dimensions.

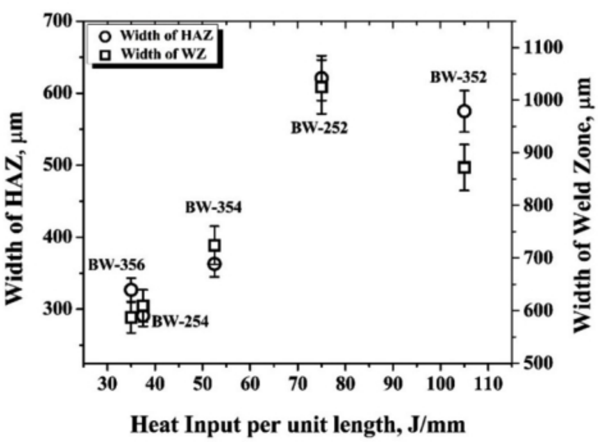

Fig. 2 : Variation of average widths of HAZ and WZ with Heat Input

Microstructure in the trough section of as received DP 600 is shown in **Fig. 3**. Uniform distribution of martensite in the matrix of ferrite is observed in **Fig. 3**. This steel has a 15 -18% average volume fraction of martensite phase embodied in ferrite matrix with an average grain size 8-11 μm. The average hardness of the base material is 180-200 HV.

Fig. 4 (i and **ii)** show the optical micrograph of HAZ and weld zone at the beam power of 2500 W and 3500 W respectively and at different welding speeds i.e., (a&b) 2000 mm/min; (c&d) 4000 mm/min, and (e&f) 6000 mm/min. Weld zone of all the weld beads produced at two different beam powers and all the welding speeds have predominantly martensite phase. Solidification of the liquid metal and solid phase transformation phenomena are involved in the weld zone formation. Formation of martensite in the weld zone that are attributed to the rapid cooling rates associated with the weld zone were much above the critical cooling rate of martensitic phase transformation for the given composition [16].

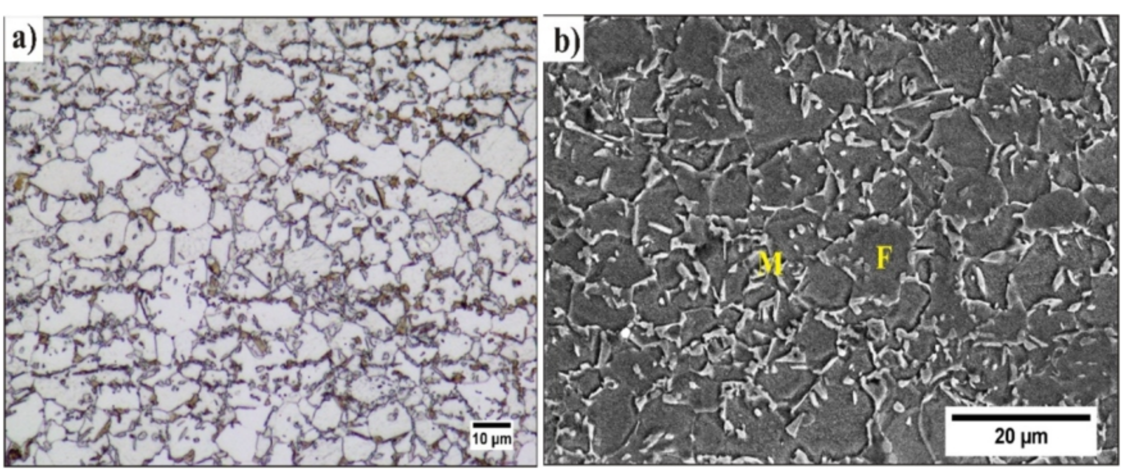

Fig. 3 : Base material microstructure of DP 600 (a) Optical Micrograph (b) SEM micrograph

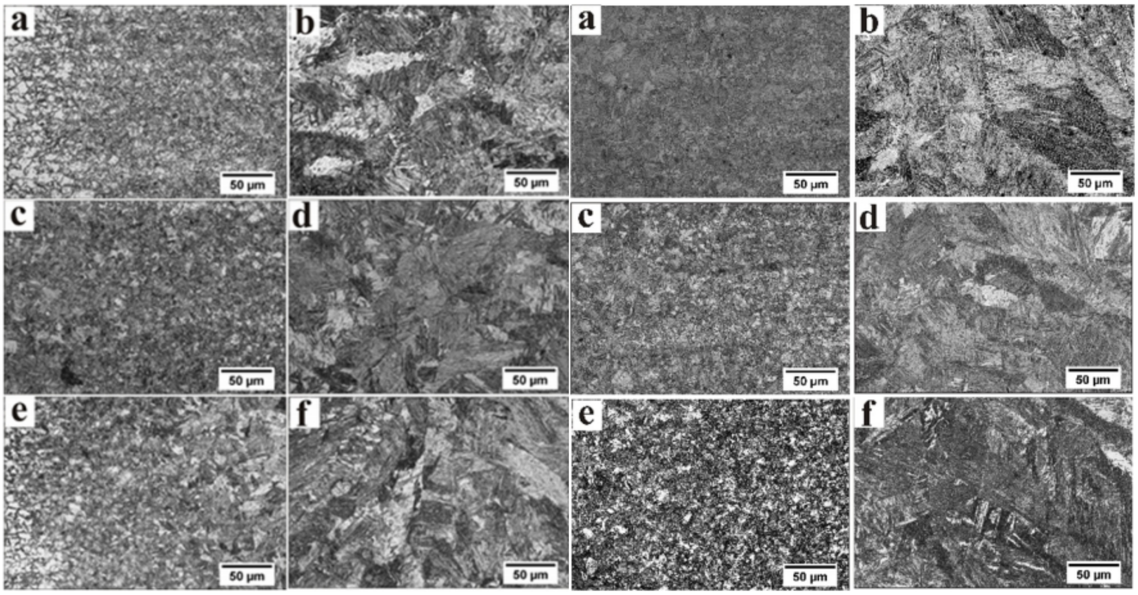

Fig. 4 : Microstructure of HAZ and Weld Zone of Beam Power (i) 2500 W and (ii) 3500 W [(a&b) TS - 2000mm/min, (c&d) TS 4000 mm/min, (e&f) TS 6000 mm/min] [a,c & e: Heat Affected Zone, b,d & f: Weld Zone]

As the heat energy is dissipated to the adjacent material during the solidification of the weld zone, the temperature of the adjacent zone has been raised to austenitic transformation temperatures (A3 and A1) and upon cooling, austenite has been transformed to martensite and ferrite, and Heat Affected Zone has been formed. The peak temperature of the material has decreased as the distance from the weld zone increased. During cooling from this peak temperature (austenite transformation temperatures) austenite has been transformed to martensite and the volume fraction of martensite is decreased as the distance from the weld zone has increased, as shown in **Fig. 5**. The zone adjacent to the fusion zone, called as inner HAZ, is exposed to the austenitic region and transforms to martensite as a predominant phase and the zone adjacent to the base material, called as outer HAZ, is exposed to intercritical temperature zone where both martensite and ferrite have been formed.

From **Fig. 6**, it is observed that martensite packet size is larger in WZ compared to the HAZ. During solidification of the weld zone, the formation of prior austenitic grains has taken place initially and martensitic transformation due to rapid solidification has been taken place within these prior austenitic grains. Whereas, solid phase transformation is involved in the HAZ, the packets of martensite have been confined to the grain

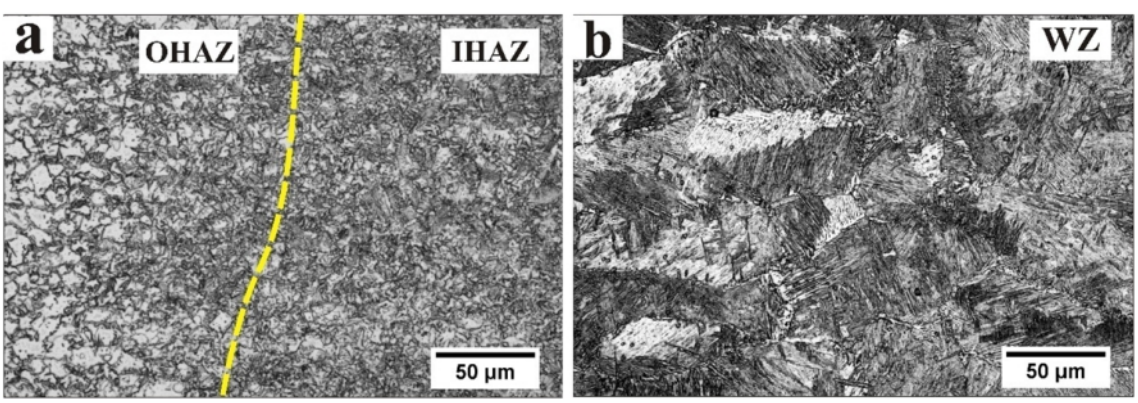

Fig. 5 : Optical Microstructure of HAZ of BW-252 showing Inner HAZ, outer HAZ and Weld Zone (OHAZ – Outer HAZ; IHAZ – Inner HAZ; WZ – Weld Zone) [(a) Heat Affected Zone, (b) Weld Zone]

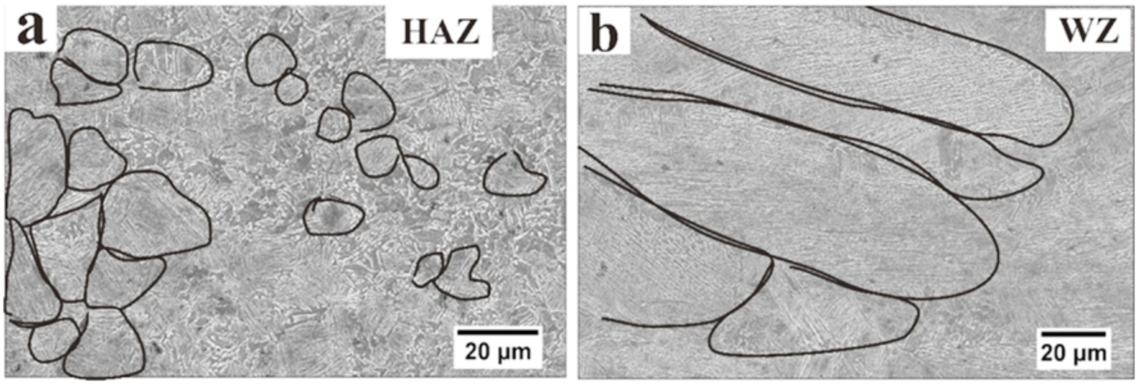

Fig. 6 : SEM Images of HAZ and WZ BW-252 [(a) HAZ, (b) WZ]

growth of austenite during heating. The size of the martensite packed has been decreased as the distance from the weld zone has increased.

Fig. 7 (a) and **(b)** show hardness profile of Vicker's hardness (HV) against distance from center for beam power of 2500 W and 3500 W respectively. From these graphs, it is observed that the average hardness of the base material is 190 ± 10 HV and that of weld zone is 360 ± 10 HV. The higher hardness in the weld zone has been attributed to the presence of martensite phase. A decrease in the hardness has been observed in the HAZ region as the proportion of martensite has been decreased with an increase in the distance from the weld zone.

Though the columnar grains in the weld zone are coarser compared to the HAZ, the laths of martensite within the grain are quite thin and closely formed (**Fig. 6b**) and are the cause for the increased hardness in the Weld Zone [17].

4.0 CONCLUSIONS

Laser beam weld beads were produced on DP 600 steel sheet and the influence of beam power and welding speed on the weld geometry, weld joint dimensions, and variation of microstructural and mechanical characteristics were studied.

- The macrostructure of the weld joint in transverse direction revealed that the weld joints were free from defects like micropores, cracks etc.
- Complete depth of penetration was observed with all the weld beads except weld bead produced with the beam power of 2500 W and 6000 mm/min. Heat input per unit length of this weld bead (25 J/mm) was not enough to melt down the material sufficient to give complete penetration.
- Welding speed has a greater influence on width of Heat Affected Zone and weld zone than laser beam power. At a

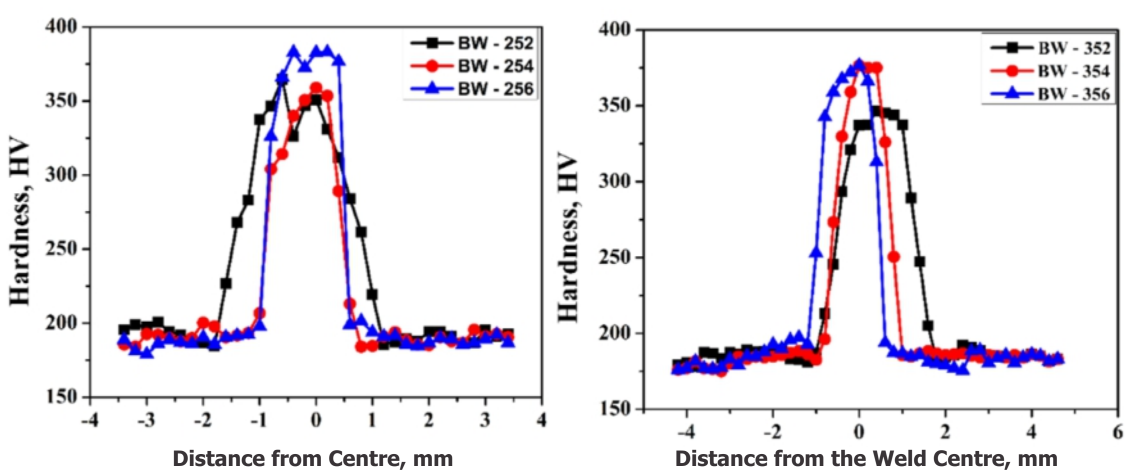

Fig. 7 : Microhardness of Bead on Plate welded structures
[(a) Hardness profile of 2500 Beam Power, (b) Hardness Profile of 3500 W beam Power]

beam power of 2500 W with an increase in the traverse speed, the width of weld joints has decreased to half. Similar behaviour has been observed with the beam power of 3500 W.

- The microstructure of the weld zone composed of large grains of lath martensite. The laths of the martensite were parallel to each other and were closely formed. The microstructure of HAZ consists of small grain size of martensite along with ferrite phase.
- An increase in the hardness of the Weld zone was observed from the base material and the increase was due to the formation of martensite in the fusion zone and the laths of the martensite are more closely formed than that in the HAZ zone.

ACKNOWLEDGMENTS: Authors would like to thank technical staff of DoAMP of DRDL and MJG of DMRL and technical staff of MGIT for their support in welding experiments and characterization of the materials.

The present paper is a revised version of an article presented in the International Congress (IC-2017) of the International Institute of Welding held in Chennai on December 07-09-2019 and organized by The Indian Institute of Welding.

REFERENCES

[1] Keeler S and Kimchi M (2014); Advanced High Strength Steels– Application Guidelines, Version 5.0, World Auto Steels.

[2] Bhattacharya D (2014); Microalloyed steels for the automotive industry technology, Metal. Mater. Miner., 11(4), pp.371-383.

[3] Schemmann L, Zaefferer S, Raabe D, Friedel F and Mattissen D (2015); Alloying effects on microstructure formation of dual phase steels, Acta Materialia, 95, pp. 386–398.

[4] Rashid MS (1981); Dual phase steels, Ann. Rev. Mater. Sci., 11, pp. 245-266.

[5] Kim S and Lee S (2000); Effects of martensite morphology and volume fraction on quasi-static and dynamic deformation behavior of dual- phase steels, Metallurgical and Materials Transactions A, 31(A), p.1753.

[6] Zhao YY, Zhangand YS and Hu W (2013); Effect of welding speed on microstructure, hardness and tensile properties in laser welding of advanced high strength steel, Science and Technology of Welding and Joining, 18(7), p. 581.

[7] ASM Metals Handbook, Volume – 6 Welding, Brazing, and Soldering.

[8] Becker F, Brettschneider C, Kallage P and Wolfram Rath (2014); Fibre lasers - a universal tool for industrial production, Laser Technik Journal.

[9] Walsh CA (2002); Laser Welding- Literature Review, Materials Science and Metallurgy Department, University of Cambridge, England.

[10] Zhengwei GU, Sibin YU, Lijun HAN, Xin LI and Hong XU (2012); Influence of welding speed on microstructures and properties of ultra-high strength steel sheets in laser welding, ISIJ International, 52(3), pp. 483–487.

[11] Santillan A, Esquivel, Nayak SS, Xia MS and Zhou Y (2012); Microstructure, hardness and tensile properties of the fusion zone in laser welding of advanced high Strength steels, Canadian Metallurgical Quarterly, 51(3).

[12] Takehide S (2001); Physical metallurgy of modern high strength steel sheets, ISIJ International, 41(6), pp. 520–532.

[13] Palov S, Viliam H and Alexander S (2014); Study of laser welding of HTC600X dual phase steels, Scientific Proceedings, 22, pp. 92-97.

[14] Pavol Š, Alexander S, Viliam H and Tomáš C (2015); Fibre laser welding of dual phase steels, Acta Metallurgica Slovaca, 21(4), pp. 311-320.

[15] Hafez KM, Ramadan M, Fathy N and Ismail M (2017); Microstructure and mechanical properties of laser welded dual phase and mild steel jointsfor automotive applications, Applied Mechanics and Materials, 865, pp. 81-87.

[16] Alves P, Lima MSF, Raabe D and Sandim HRZ (2017); Laser beam welding of dual-phase DP 1000 Steel, Journal of Material proceeding Tech., 252, pp. 498-510.